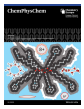

Cyclic Octamer of Hydroxyl-functionalized Cations with Net Charge $Q = +8e$ Kinetically Stabilized by a 'Molecular Island' of Cooperative Hydrogen Bonds

Jule Kristin Philipp,[a] Sebastian Fritsch,[a] and Ralf Ludwig*[a, b, c]

Cyclic octamers are well-known structural motifs in chemistry, biology and physics. These include covalently bound cyclic octameric sulphur, cylic octa-alkanes, cyclo-octameric peptides as well as hydrogen-bonded ring clusters of alcohols. In this work, we show that even calculated cyclic octamers of hydroxy-functionalized pyridinium cations with a net charge $Q = +8e$ are kinetically stable. Eight positively charged cations are kept together by hydrogen bonding despite the strong Coulomb repulsive forces. Sufficiently long hydroxy-octyl chains prevent "Coulomb explosion" by increasing the distance between the positive charges at the pyridinium rings, reducing the Coulomb repulsion and thus strengthen hydrogen bonds between the OH groups. The eightfold positively charged cyclic octamer shows spectroscopic properties similar to those obtained for hydrogen-bonded neutral cyclic octamers of methanol. Thus, the area of the hydrogen bonded OH ring represents a 'molecular island' within an overall cationic environment. Although not observable, the spectroscopic properties and the correlated NBO parameters of the calculated cationic octamer support the detection of smaller cationic clusters in ionic liquids, which we observed despite the competition with ion pairs wherein attractive Coulomb forces enhance hydrogen bonding between cation and anion.

1. Introduction

In hydroxyl-functionalized ionic liquids (ILs) hydrogen bonding has a double-faced nature. Two distinct types of hydrogen bonds (H-bonds) coexist: The conventional H-bonds in ion pairs between cation and anion enhanced by attractive Coulomb interaction, and the elusive H-bonds between like-charged ions that are supposed to be much weaker due to the repulsive Coulomb force.[1–5] Despite this expectation, the hydrogen bonds in cationic clusters are evidently stronger than the ones in ion pairs as shown by stronger redshifted OH vibrational bands in IR spectra.[6] Consequently, we detected cationic clusters in the bulk liquid as well as in the gas phase by spectroscopic methods.[7–14] We observed significantly enhanced cationic cluster formation for hydroxyl-functionalized ILs (*n*-hydroxyalkyl)-pyridinium bis(trifluoromethanesulfonyl)imide $[HO–(CH_2)_n–Py][NTf_2]$. These ILs comprise polarizable pyridinium cations, weakly interacting anions and sufficiently long hydroxyl-alkyl chains ($n = 4$) at the cation for tethering the positively charged pyridinium ring away from the hydroxy group, allowing hydrogen bonding between the OH groups of the like-charged ions. The question arises whether pure cationic clusters $[HO–(CH_2)_n–Py^+]_m$ can exist without the mediating 'solvent effects' by polarizable cations or weakly interacting counterions. The only parameter left for tuning the strength of the Coulomb interaction is lengthening of the hydroxyalkyl chains for reducing the repulsive Coulomb forces and thus enhancing hydrogen bonding. Recently, we explored quantum chemical calculations for studying the stability of cationic dimers $[HO–(CH_2)_n–Py^+]_2$.[15] Although we could significantly decrease the Coulomb repulsion, very long hydroxy-alkyl chains with $n = 15$ were needed before meta-stable dimers changed into stable dimers, wherein the Coulomb repulsion is fully compensated by the attractive hydrogen bond. Depending on the alkyl chain length, we could also calculate larger cationic clusters up to cyclic pentamers and hexamers.[16] Taking dispersion effects into account we found minimum structures for the cyclic pentamer $[HO–(CH_2)_2–Py^+]_5$ and even for the cyclic hexamer $[HO–(CH_2)_3–Py^+]_6$ due to slightly longer hydroxyalkyl chains in the latter (see Figure 1a,b). In the meta-stable clusters with net charges $Q = +5e$ and $Q = +6e$ Coulomb repulsion is significantly decreased for the benefit of stronger hydrogen bonds. The structural motifs of the calculated cationic clusters very much resemble the cyclic pentamers and hexamers as observed experimentally for water and alcohols.[17–21] Although the structural motifs of the molecular and ionic clusters were similar, intra- and intermolecular bond lengths as well as spectroscopic properties of the multiply charged clusters were still influenced by the strong repulsive

[a] B. Sc. J. K. Philipp, B. Sc. S. Fritsch, Prof. Dr. R. Ludwig
Universität Rostock, Institut für Chemie, Abteilung Physikalische und Theoretische Chemie, Dr.-Lorenz-Weg 2, 18059 Rostock, Germany
E-mail: ralf.ludwig@uni-rostock.de
[b] Prof. Dr. R. Ludwig
Universität Rostock, Department LL&M, Albert-Einstein-Str. 25, 18059 Rostock, Germany
[c] Prof. Dr. R. Ludwig
Leibniz-Institut für Katalyse an der Universität Rostock e.V., Albert-Einstein-Str. 29a, 18059 Rostock, Germany

Supporting information for this article is available on the WWW under https://doi.org/10.1002/cphc.202000681

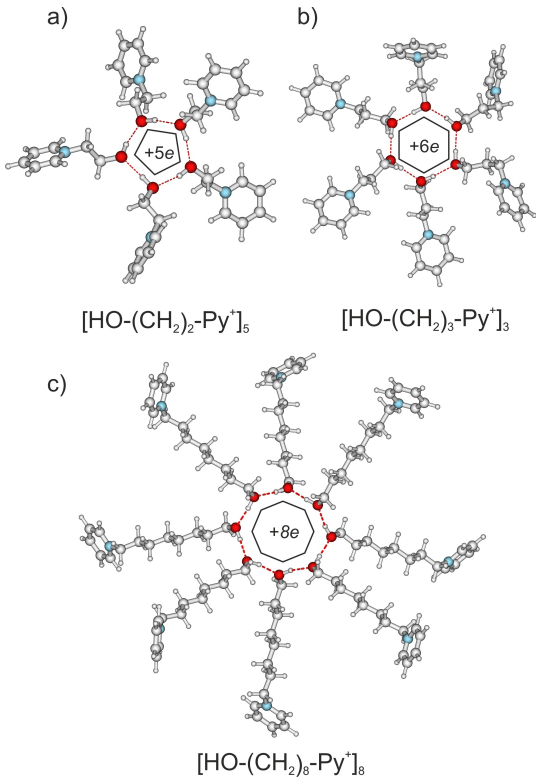

Figure 1. The largest meta-stable cationic clusters obtained from B3LYP-D3/6-31 + G* calculations: a) the cyclic pentamer $[HO–(CH_2)_2–Py^+]_5$, with net charge $Q = +5e$, b) the cyclic hexamer $[HO–(CH_2)_3–Py^+]_5$ with net charge $Q = +6e$ and c) the cyclic octamer $[HO–(CH_2)_8–Py^+]_8$ with net charge $Q = +8e$.

Coulomb forces. The hydrogen bonds were weaker and the spectroscopic probes such as NMR proton chemical shift less downfield shifted compared to similar sized and structured molecular clusters.[22–24] Calculating even larger cationic clusters seemed challenging for two reasons. Firstly, each additional positive charge would further increase the repulsive Coulomb interaction. Secondly, it is well-known for molecular clusters that the cooperative hydrogen bonding is maximized in cyclic hexamers and that larger clusters are entropically disfavored.

It is the purpose of this work to find larger meta-stable cationic clusters, wherein, in the absence of any mediating "solvent effects" by counterions, cooperative hydrogen bonding essentially compensate the repulsive Coulomb forces. In particular we were interested in cyclic octamers exhibiting the largest net charge $Q = +8e$ ever reported for hydrogen bonded cationic clusters so far (see Figure 1c). Here, we show that "Coulomb explosion" is preventable when the cations have long hydroxyl-octyl chains significantly reducing the repulsive forces and enhancing hydrogen bonding between the hydroxyl groups at the same time. The calculated bond lengths and spectroscopic observables of cationic clusters $[HO–(CH_2)_8–Py^+]_m$ with $m = 2–8$ are similar to those of molecular clusters of methanol. Obviously, the meta-stability of these clusters originate from 'molecular islands' of H-bonded structural motifs embedded in an overall strongly cationic environment.

We have chosen clusters of the hydroxy-functionalized cations 1-(*n*-hydroxyalkyl)pyridinium $[HO–(CH_2)_m–Py^+]$ with $n = 2,3$, and 8 as model systems. We calculated monomers, dimers ($m = 2$) and cyclic clusters up to octamers ($m = 8$). The hydroxy groups on the cations form hydrogen bonds and promote the aggregation into highly charged cationic clusters. For comparison between cationic and molecular clusters we calculated same sized and shaped clusters of methanol molecules $(OH–CH_3)_m$ with $m = 1–8$. We employed B3LYP/6-31 + G* and B3LYP-D3/6-31 + G* calculations performed with the Gaussian 09 program and analyzed with the NBO 6.0 program.[25–27] For calculating all cationic and molecular clusters at the same level of theory, we used the well-balanced 6-31 + G* Pople basis set.[25] Including polarization as well as diffuse functions, this basis set is suitable for reasonably calculation of hydrogen-bonded clusters of like-charged ions.[3–6] The relatively small 6-31 + G* basis set needs to be used also for better comparison with earlier studies of molecular and ionic clusters.[22–24] We demonstrated that the salient properties of these clusters can be robustly calculated with both smaller und larger basis sets so long Grimme's D3 dispersion correction is considered.[28–30] This is demonstrated for the features of the largest cationic cluster found here (see calculated cyclic octamers revealed from B3LYP-D3 calculations at 3-21G, 6-31G* and 6–31 + G* basis sets (see **SI**). All pure cationic clusters $[HO–(CH_2)_n–Py^+]_m$ and molecular clusters $[HO–CH_3]_m$ were fully optimized. The calculated vibrational frequencies were all positive, showing that we calculated at least local minimum structures. For all geometry-optimized cationic and molecular clusters, we calculated the hydroxy proton chemical shifts, δ ^{1}H as sensitive probes for hydrogen bonding. These NMR spectroscopic observables are related to NBO-calculated second order stabilization energy $\Delta E(2)_{n\rightarrow\sigma^*}$, and charge transfer, q_{CT}.[26,27]

2. Cyclic Clusters up to Net Charge $Q = +8e$

First, we optimized the dimer and cyclic cationic clusters $[HO–(CH_2)_n–Py^+]_m$ up to octamers ($m = 2–8$) (see **SI**). For comparison with molecular clusters showing similar size and shape, we calculated molecular clusters of methanol $[OH–CH_3]_m$ with $m = 2–8$. For both the cationic and the molecular systems, the starting geometries of linear trimers, tetramers and pentamers were optimized towards cyclic clusters, wherein cooperative H-bonding is maximized. Including dispersion correction, we obtained intrinsic meta-stable cyclic trimers, tetramers, pentamers, hexamers and finally the desired cyclic octamer $[HO–(CH_2)_8–Py^+]_8$ which exhibits a net charge of $Q = +8e$. The meta-stable cationic clusters resemble the cyclic clusters of methanol $[HO–CH_3]_n$ and those known for other alcohols and water.[22–24] For better understanding the role of hydrogen bonding in the cationic clusters and how it behaves with increasing hydroxylalkyl chain length, we also discuss the earlier calculated cationic clusters $[HO–(CH_2)_2–Py^+]_m$ and $[HO–(CH_2)_3–Py^+]_m$, respectively.

For demonstrating the meta-stability of the cationic clusters $[HO–(CH_2)_n–Py^+]_m$ with increasing alkyl chain length (n = 2,3,8),

we show the calculated energies per cation in Figure 2. For $[HO–(CH_2)_2–Py^+]_m$ the energies increasing from 75 kJ mol^{-1} for the dimer up to 250 kJ mol^{-1} for the cylic pentamer, which is only meta-stable if dispersion forces are taken into account. Otherwise, only dimers can be calculated and larger clusters dissociate. We showed recently that increasing the alkyl chain length by one methylene group already allows achieving cyclic hexamers. Without dispersion correction, only cylic pentamers are meta-stable. Thus, Grimme's dispersion correction accounts for one additional hydrogen bond pushing the meta-stability from cyclic pentamers to cyclic hexamers. It seems that the critical threshold for meta-stability of the cationic clusters per species is 260 kJ mol^{-1}.(see Figure 2) We also tried to calculate cationic clusters with longer hydroxyalkyl chains $n=4$, 5, 6, but could never optimize structures larger than the cyclic hexamers already obtained for $[HO–(CH_2)_3–Py^+]$. The cyclic hexamers for alkyl chains $n=4$, 5, 6 had energies per cation below 260 kJ mol^{-1} and showed meta-stability, whereas larger clusters such as cyclic octamers exceeded this threshold and dissociated. As shown in Figure 2, we had to increase the alkyl chain length up to $n=8$ in order to achieve meta-stable cyclic octamers $[HO–(CH_2)_8–Py^+]_8$. In this cyclic octamer the energy per cation is dropped down to 180 kJ mol^{-1} well below the threshold. This energy is low enough to overcome the entropic penalty by adding two cations to the cyclic hexamer. Cooperative hydrogen bonding stabilizes the cyclic octamer, which resembles H-bond structural motifs known from cyclic alkanes or molecular clusters as shown here for methanol. The H-bond configuration of the cyclic octamer is crown like and mimics the second most stable cyclic alkane (see Figure 3).[30] That covalent bonds and hydrogen bonds result in similar structures may be attributed to the covalent character of hydrogen bonding.[31] The cyclic octamer is not planar as suggested by the 2-D plot in Figure 1c. The pyridinium rings in the cyclic cationic octamer try to increase the distances to each other for minimizing the repulsive Coulomb forces. The three-dimensional structure is built by two truncated pyramids with square bases rotated against each other by 45 degrees and sitting opposite to each other. The square surfaces twisted against each other form the octameric H-bonded ring (see Figure 3).

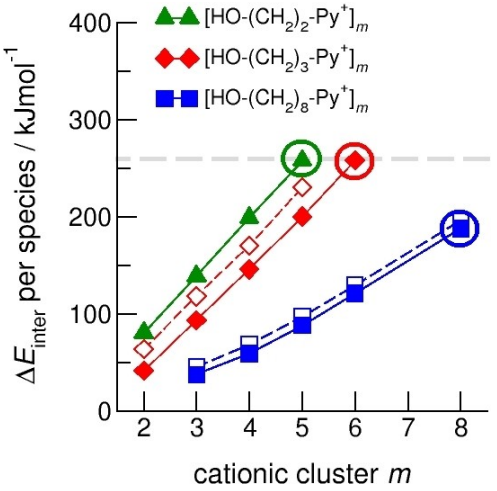

Figure 2. Intermolecular energies per species in the cationic clusters $[HO–(CH_2)_2–Py^+]_m$, (green triangles), $[HO–(CH_2)_3–Py^+]_m$ (red diamonds) and $[HO–(CH_2)_8–Py^+]_m$, (blue squares) respectively. The filled symbols indicate the calculated energies for considering dispersion forces. Only the cationic clusters with energies below 260 kJ mol^{-1} per cation are meta-stable. The others undergo 'Coulomb explosion' and dissociate.

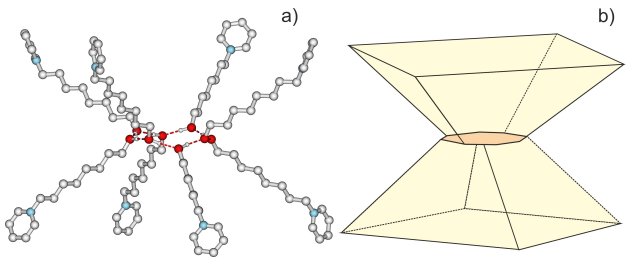

Figure 3. The calculated three-dimensional cyclic octamer $[HO–(CH_2)_8–Py^+]_8$ with net charge $Q=+8e$. b) Two truncated pyramids rotated against each other by 45 degrees are standing opposite to each other. The twisted square surfaces form the H-bonded cyclic octamer.

3. Intra- and Intermolecular Bond Lengths of Cationic and Molecular Clusters

In the cationic clusters, the charge transfer from the oxygen lone pair orbital into the OH antibonding orbital results in hydrogen bonding such as in molecular clusters but less pronounced. However, even in the eightfold H-bonded cationic cluster with $Q=+8e$ cooperative hydrogen bonding attenuates the repulsive Coulomb interaction, resulting in longer intra- and shorter intermolecular bond lengths. Despite strong electrostatic opposition, the cationic clusters show typical H-bond distances and spectroscopic signatures as known for molecular liquids. The intramolecular bond lengths, R(OH), and the intermolecular bond distances, R(H···O) and R(O···O) of the cationic clusters $[HO–(CH_2)_2–Py^+]_m$, $[HO–(CH_2)_3–Py^+]_m$, and $[HO–(CH_2)_8–Py^+]_m$, are shown along with those of the methanol clusters $[HO–CH_3]_m$ in Figure 4. Stronger hydrogen bonds are reflected in elongated R(OH) covalent bonds, and shortened R(H···O) and R(O···O) hydrogen bonds. It is well-known from the literature that cooperative hydrogen bonding is saturated in the cyclic hexamer.[32,33] Larger ring structures are slightly weaker bound as shown here for the intra and inter molecular geometries. Here, we take the geometries of the methanol clusters as reference for hydrogen bonded molecular systems. In principle, the cationic clusters $[HO–(CH_2)_2–Py^+]_m$ show the same tendencies with increasing cluster size. Although the cyclic pentamer is meta-stable, the maximum hydrogen bond strength is achieved in the cyclic tetramer. The same sized clusters $[HO–(CH_2)_3–Py^+]_m$ show further enhanced hydrogen bonding attributed to further lengthened intramolecular OH bonds and shortened intermolecular distances R(H···O) and R(O···O) distances. Compared to the molecular system, hydrogen bonding is less pronounced in the cationic clusters, nevertheless we observe typical cooperative behaviour of hydrogen

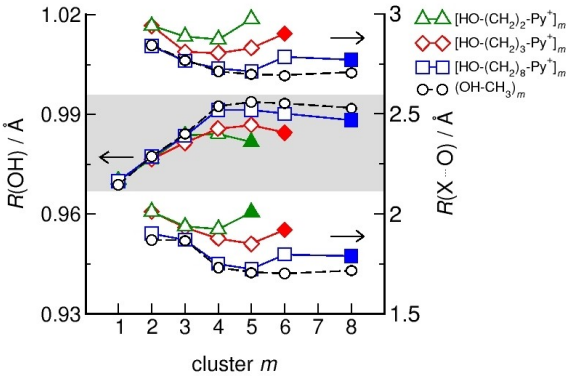

Figure 4. The intramolecular bond lengths, *R*(OH) (left axis, grey bar) and the intermolecular bond distances, *R*(H···O) and *R*(O···O) (right axis) are shown for the cationic clusters $[HO–(CH_2)_2–Py^+]_m$ (green triangles), $[HO–(CH_2)_3–Py^+]_m$ (red diamonds) and $[HO–(CH_2)_8–Py^+]_m$ (blue squares) along with the corresponding geometries of methanol clusters $[HO–CH_3]_m$ (black circles). The largest meta-stable cluster for each cation is indicated by filled symbols.

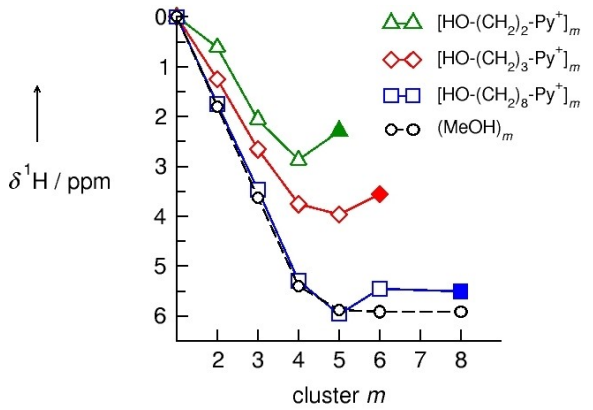

Figure 5. Calculated average NMR proton chemical shifts, δ ^{1}H, of the hydroxyl protons for the cationic clusters $[HO–(CH_2)_2–Py^+]_m$ (green triangles), $[HO–(CH_2)_3–Py^+]_m$ (red diamonds) and $[HO–(CH_2)_8–Py^+]_m$ (blue squares) along with the corresponding chemical shifts of methanol clusters $[HO–CH_3]_m$ (black circles). The largest meta-stable cationic cluster for each cation show the strongest downfield shift (filled symbols). It is interesting to note that the chemical shifts of the cationic clusters $[HO–(CH_2)_8–Py^+]_m$ and the methanol clusters $[HO–CH_3]_m$ are almost identical indicating a 'molecular island' within the cationic environments.

bonding despite the strong repulsive forces. In the cationic clusters $[HO–(CH_2)_8–Py^+]_m$ the positive charge centres at the pyridinium ring are so far away (~12 Å) away from the OH groups that the latter can easily form hydrogen bonds among each other. The Coulomb repulsion in these clusters is weak and the hydrogen bonds are almost as strong as in the molecular system. This behaviour continues to the cyclic pentamer and only slightly changes for the larger cyclic hexamer and octamer. Obviously, the weak like-charge repulsion in cationic clusters $[HO–(CH_2)_8–Py^+]_m$ allows the formation of 'molecular islands' wherein hydrogen bonds are as strong as in molecular systems.

4. Spectroscopic Observables of Cationic and Molecular Clusters

The existence of 'molecular islands' is even better illustrated by the calculated NMR δ^1H proton chemical shifts of the hydroxyl groups, which are sensitive probes of hydrogen bonding. In Figure 5 we show the δ^1H values for the cationic clusters $[HO–(CH_2)_2–Py^+]_m$, $[HO–(CH_2)_3–Py^+]_m$, and $[HO–(CH_2)_8–Py^+]_m$, as well as for the methanol clusters $[HO\text{-}CH_3]_m$, all referenced versus the corresponding values of the non-bonded monomers. The proton chemical shifts are downfield shifted with increasing hydrogen bond strength and show the same tendencies as the cluster geometries. The maximum downfield shifts of the hydroxy protons within the cationic clusters are about 3 ppm for $[HO–(CH_2)_2–Py^+]_m$, 4 ppm for $[HO–(CH_2)_3–Py^+]_m$, and 6 ppm for $[HO–(CH_2)_8–Py^+]_m$.

We surprisingly observed that the proton chemical shifts of the $[HO–(CH_2)_8–Py^+]_m$ clusters are as strongly downfield shifted as those of similar sized methanol clusters (~6 ppm).[22–24] The attractive hydrogen bonds in the cationic clusters are obviously fully developed and no more weakened by the repulsive Coulomb forces. Although cationic clusters have significantly positive energies, strong hydrogen bonds partially compensate the repulsive Coulomb forces leading to meta-stable structures. In clusters $[HO–(CH_2)_8–Py^+]_m$ the positive charge centres at the pyridinium rings are that far away from each other and from the hydroxyl groups that a 'molecular island' is created, wherein, the hydrogen bonds can formed similarly as in a purely molecular system. For the first time we can report, that such a 'molecular island' is able to exist in a general cationic environment.

5. NBO Parameters and Spectroscopic Observables of the Cationic and Molecular Clusters

The hydrogen bonds between hydroxyl groups in cationic clusters, OH···OH, are characterized by donation of electron density from the oxygen lone pair orbital of one cation into the OH antibonding orbital of a second cation. The resulting larger negative charge at the OH oxygen of the latter can then be transferred into the OH antibonding orbital of another cation, further enhancing hydrogen bonding. This process leads to even stronger cooperativity in the cyclic structures such as tetramers, pentamers, hexamers or even octamers as shown here. This way, the short-range donor-acceptor covalency forces attenuate the strong long-range electrostatic repulsive forces as expected for ions of like charge. These features can be best rationalized in the framework of the natural bond orbital (NBO) analysis.[26,27] NBO analysis shows typical strong $n_o \rightarrow \sigma^*_{OH}$ donor-acceptor interaction, corresponding to second order stabilization energies $\Delta E(2)_{n\rightarrow\sigma^*}$ and estimated total charge transfers of q_{TC} for the enhanced OH···OH hydrogen bonds, respectively. These typical NBO descriptors are plotted versus δ^1H downfield

chemical shifts of all cationic and molecular clusters. We show in Figure 6 that the spectroscopic probe of hydrogen bonding is linearly related to both NBO descriptors. Obviously, spectroscopic and NBO descriptors characterize hydrogen bonding and cooperativity in the same way. The downfield proton chemical shifts are related to increasing stabilization energies, $\Delta E(2)_{n\rightarrow\sigma^*}$, and enhanced charge transfer, q_{CT}. That the strongest intermolecular stabilization energies are found for the cyclic structures is well correlated to the cooperative binding energies and chemical shifts. These 'closed-CT' ring structures have high stability, characterized by strong hydrogen bonds and strongly downfield shifted chemical shifts. Both NBO descriptors reflect the downfield shifts of the hydroxy protons within the cationic clusters. Stabilization energies $\Delta E(2)_{n\rightarrow\sigma^*}$ of about 15 kJ mol^{-1}, 20 kJ mol^{-1}, and 30 kJ mol^{-1} for the largest clusters $[HO–(CH_2)_2–Py^+]_5$, $[HO–(CH_2)_3–Py^+]_6$ and $[HO–(CH_2)_8–Py^+]_8$ correspond to maximum 3, 4 and 6 ppm NMR proton downfield shifts. The NBO parameters $\Delta E(2)_{n\rightarrow\sigma^*}$ and q_{TC} suggest similar NMR chemical shifts of the hydroxyl protons, independently whether the OH groups belong to cationic or molecular clusters. Thus, the NBO descriptors support the existence of a 'molecular island' in cationic clusters, wherein hydrogen bonds are as strong as in molecular clusters of methanol.

6. Conclusion

In this work we show that ring clusters of monovalent hydroxyl-functionalized cations $[HO–(CH_2)_8–Py^+]_m$ with net charges up to $Q=+8e$ are kinetically stable. Cooperative hydrogen bonding prevents the intrinsically meta-stable cyclic octamer $[HO–(CH_2)_8–Py^+]_8$ from 'Coulomb explosion'. The long hydroxyl-octyl chains increase the distance between the positive charge centres at the pyridinium ring and the hydroxyl groups resulting in significantly reduced Coulomb repulsion and enhanced hydrogen bonding. Intra- and inter molecular bond distances as well as NMR proton chemical shifts, both representing sensitive probes of hydrogen bonding, correspond to those calculated for methanol clusters. The NMR spectroscopic probe for hydrogen bonding for all clusters strongly correlates with the NBO-calculated stabilization energies and charge transfers. The cationic clusters $[HO–(CH_2)_8–Py^+]_8$ show almost the same bond distances and proton chemical shifts as observed for methanol clusters $[HO–CH_3]_m$. Cooperative hydrogen bonding is maximized on a 'molecular island' within an overall cationic environment.

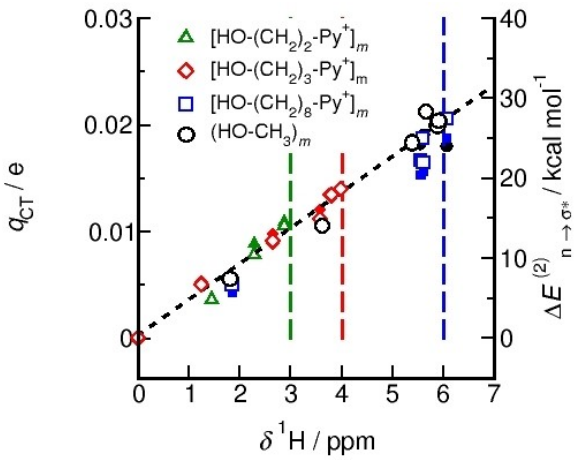

Figure 6. Average NBO-calculated second order stabilization energies $\Delta E(2)_{n\rightarrow\sigma^*}$ (open symbols) and estimated total charge transfers q_{CT} (filled symbols) for cationic clusters $[HO–(CH_2)_2–Py^+]_m$, (green triangles), $[HO–(CH_2)_3–Py^+]_m$ (red diamonds), $[HO–(CH_2)_8–Py^+]_m$,(blue squares) and methanol clusters $[HO–CH_3]_m$ (black circles). The linear dependence indicates the strong relation between NBO stabilization energies and charge transfers with spectroscopic properties, such as NMR chemical shifts. The largest downfield shifts for the cationic clusters $[HO–(CH_2)_n–Py^+]_m$ are indicated by the vertical dotted green ($n=2$), red ($n=3$) and blue ($n=8$) lines.

Acknowledgements

This work has been supported by the DFG Research Grant LU-506/14-2.

Conflict of Interest

The authors declare no conflict of interest.

Keywords: clusters of like-charged ions · Coulomb explosion · DFT calculations · hydrogen bonding · ionic liquids

[1] S. A. Katsyuba, M. V. Vener, E. E. Zvereva, Z. Fei, R. Scopelliti, G. Laurenczy, N. Yan, E. Paunescu, P. J. Dyson, *J. Phys. Chem. B.* **2013**, *117*, 9094–9105.
[2] M. Fakhraee, B. Zandkarimi, H. Salari, M. R. Gholami, *J. Phys. Chem. B* **2014**, *118*, 14410–14428.
[3] A. Knorr, K. Fumino, A.-M. Bonsa, R. Ludwig, *Phys. Chem. Chem. Phys.* **2015**, *17*, 30978–30982.
[4] A. Knorr, R. Ludwig, *Sci. Rep.* **2015**, *5*, 17505.
[5] A. Knorr, P. Stange, K. Fumino, F. Weinhold, R. Ludwig, *ChemPhysChem* **2016**, *17*, 458–462.
[6] A. Strate, T. Niemann, P. Stange, D. Michalik, R. Ludwig, *Angew. Chem. Int. Ed.* **2017**, *56*, 496–500; *Angew. Chem.* **2017**, *129*, 510–514.
[7] T. Niemann, J. Neumann, P. Stange, S. Gärtner, T. G. A. Youngs, D. Paschek, R. Atkin, R. Ludwig, *Angew. Chem. Int. Ed.* **2019**, *58*, 12887–12892; Angew. Chem. **2019**, 131, 13019–13024.
[8] A. E. Khudozhitkov, V. Overbeck, P. Stange, D. Paschek, A. G. Stepanov, D. I. Kolokolov, R. Ludwig, *Angew. Chem. Int. Ed.* **2019**, *58*, 17863–17871; Angew.Chem. **2019**,131,18027–18035.
[9] T. Niemann, D. H. Zaitsau, A. Strate, P. Stange, R. Ludwig, *Phys. Chem. Chem. Phys.* **2020**, *22*, 2763–2774.
[10] A. E. Khudozhitkov, T. Niemann, P. Stange, M. Donoshita, A. G. Stepanov, H. Kitagawa, D. I. Kolokolov, R. Ludwig, *J. Phys. Chem. Lett.* **2020**, *11*, 15, 6000–6006.
[11] F. S. Menges, H. J. Zeng, P. J. Kelleher, O. Gorlova, M. A. Johnson, T. Niemann, A. Strate, R. Ludwig, *J. Phys. Chem. Lett.* **2018**, *9*, 2979–2984.
[12] T. Niemann, A. Strate, R. Ludwig, H. J. Zeng, F. S. Menges, M. A. Johnson, *Angew. Chem. Int. Ed.* **2018**, *57*, 15364–15368; *Angew. Chem.* **2018**, *130*, 15590–15594.
[13] T. Niemann, A. Strate, R. Ludwig, H. J. Zeng, F. Menges, M. A. Johnson, *Phys. Chem. Chem. Phys.* **2019**, *21*, 18092–18098.
[14] H. Zeng, F. Menges, M. Johnson, T. Niemann, A. Strate, R. Ludwig, *J. Phys. Chem. Lett.* **2020**, *14*, 683–688.
[15] T. Niemann, P. Stange, A. Strate, R. Ludwig, *Phys. Chem. Chem. Phys.* **2019**, *21*, 8215–8220.

[16] T. Niemann, P. Stange, A. Strate, R. Ludwig, *ChemPhysChem* **2018**, *19*, 1691–1695.
[17] K. Nauta, R. E. Miller, *Science* **2000**, *287*, 293–295.
[18] K. Liu, J. D. Cruzan, R. J. Saykally, *Science* **1996**, *271*, 929–933.
[19] U. Buck, J.-G. Siebers, Richard J. Wheatley, *J. Chem. Phys.* **1998**, *108*, 20.
[20] M. I. Sulaiman, S. Yang, A. Ellis, *J. Phys. Chem. A.* **2017**, 121, 771–776.
[21] A. Malloum, J. J. Fifen, J. Conradie, *Phys. Chem. Chem. Phys.* **2018**, *20*, 29184–20206.
[22] R. Ludwig, *Phys. Chem. Chem. Phys.* **2002**, *4*, 5481–5487.
[23] K. M. Murdoch, T. D. Ferris, J. C. Wright, T. C. Farrar , *J. Chem. Phys.* **2002**, *116*, 5717.
[24] R. Ludwig, *ChemPhysChem* **2005**, *6*, 1369–1375.
[25] Gaussian 09, Revision A.02, M. J. Frisch, G. W. Trucks, H. B. Schlegel, G. E. Scuseria, M. A. Robb, J. R. Cheeseman, G. Scalmani, V. Barone, G. A. Petersson, H. Nakatsuji, X. Li, M. Caricato, A. Marenich, J. Bloino, B. G. Janesko, R. Gomperts, B. Mennucci, H. P. Hratchian, J. V. Ortiz, A. F. Izmaylov, J. L. Sonnenberg, D. Williams-Young, F. Ding, F. Lipparini, F. Egidi, J. Goings, B. Peng, A. Petrone, T. Henderson, D. Ranasinghe, V. G. Zakrzewski, J. Gao, N. Rega, G. Zheng, W. Liang, M. Hada, M. Ehara, K. Toyota, R. Fukuda, J. Hasegawa, M. Ishida, T. Nakajima, Y. Honda, O. Kitao, H. Nakai, T. Vreven, K. Throssell, J. A. Montgomery, Jr., J. E. Peralta, F. Ogliaro, M. Bearpark, J. J. Heyd, E. Brothers, K. N. Kudin, V. N. Staroverov, T. Keith, R. Kobayashi, J. Normand, K. Raghavachari, A. Rendell, J. C. Burant, S. S. Iyengar, J. Tomasi, M. Cossi, J. M. Millam, M. Klene, C. Adamo, R. Cammi, J. W. Ochterski, R. L. Martin, K. Morokuma, O. Farkas, J. B. Foresman, D. J. Fox, Gaussian, Inc., Wallingford CT, 2016.
[26] E. D. Glendening, J. K. Badenhoop, A. E. Reed, J. E. Carpenter, J. A. Bohmann, C. M. Morales, C. R. Landis, F. Weinhold, *NBO 6.0.* Theoretical Chemistry Institute, University of Wisconsin, Madison (**2013**).
[27] F. Weinhold, C. R. Landis, *Valency Bonding A Natural Bond Orbital Donor-Acceptor Perspective*, Cambridge, University Press, Cambridge, **2005**.
[28] S. Grimme, J. Antony, S. Ehrlich, H. Krieg, *J. Chem. Phys.* **2010**, *132*, 154104.
[29] S. Ehrlich, J. Moellmann, W. Reckien, T. Bredow, S. Grimme, *ChemPhysChem* **2011**, *12*, 3414–3420.
[30] S. Grimme, A. Jansen, *Chem. Rev.* **2016**, *116*, 5105–5154.
[31] W. R. Rocha, J. R. Pliego Jr., S. M. Resende, H. F. Dos Santos, M. A. De Oliveira, W. B. De Almeida, *J. Comput. Chem.* **1998**, *19*, 524–534.
[32] F. Weinhold, E. D. Glendening, *J. Phys. Chem. A* **2018**, *122*, 724–732.
[33] S. S. Xantheas, T. H. Dunning, *J. Chem. Phys.* **1993**, *99*, 8774–8792.

Manuscript received: August 3, 2020
Revised manuscript received: August 20, 2020
Accepted manuscript online: August 26, 2020
Version of record online: September 28, 2020